The Ocean Engineering Committee

Committee Chairman: Dr. Carl Trygve Stansberg
Session Chairman: Ir. George F.M. Remery

1. DISCUSSIONS

1.1 Discussion to the 24th ITTC Ocean Engineering Committee by Neil Bose, Memorial University of Newfoundland, Canada

The Committee showed a picture of a floating wind farm with sails. Can you comment on the use of the sails on this farm?

The Committee explained that wind production in ocean engineering basins has many problems. Can the Committee comment as to how wind production and wind forces modelling can be improved in these facilities?

1.2 Discussion to the 24th ITTC Ocean Engineering Committee by Bruce Johnson, U.S. Naval Academy, USA

I congratulate the Ocean Engineering Committee on their comprehensive Report.

There is an ongoing development in field wave measurements which you may want to monitor and briefly summarize the state of the art for the 25th ITTC.

The EU MaxWave project is encouraging the development of an X-Band wave radar post processor to show the operator a spatial view of the wave field out to about a 2 kilometre radius, depending on the height of the wave radar. The German developed WaMosII system, for example, averages 32 sweeps of the radar and displays various wave characteristics both numerically and visually. An estimate of the time dependent significant wave height and period in the measured portion of the wave field is calculated and displayed, along with other characteristics which are nearly impossible to determine using only single point wave measurements. One of the most interesting visuals includes the distance to and direction of travel of three-dimensional wave groups, which form and disappear because of energy concentrations and dispersal. Such special descriptions offer the possibility of estimating the probabilities of occurrence of wave groups and rogue waves which are rarely measured by single point wave measurements.

Such a system should eventually give the master and helmsman operator guidance in terms of avoiding ship motions which impair ship operations, for example helicopter operations, slamming situations and dangerous rolls for those engaged in deck operations.

1.3 Discussion to the 24th ITTC Ocean Engineering Committee by Martin Renilson, QinetiQ, United Kingdom

Firstly, I would like to thank the Committee for a very interesting Report.

I was particularly interested in the comments on the evolution of a narrow-band spectrum. Interesting figures were shown in the presentation, but they are not in the Report. It would add considerably if these could be included, along with an explanation in the discussion.

The Report refers to the fact that this can be predicted numerically by a non-linear model, however there are no details of this model, nor any actual quantitative comparisons given. I would really appreciate further details of this model, and quantitative comparison to justify the comments in the Report.

1.4 Discussion to the 24th ITTC Ocean Engineering Committee by Yanying Wang and Kun Qian, Dalian University of Technology, China, on a Numerical Simulation of Waves by use of the NURBS based BEM Method

By using the mixed Eulerian-Lagrange method, the free surface boundary condition is satisfied on the instant free surface and on body surface in this computation. The standard 4th order Adams-Bashforth-Moulton method and the 4th order Runge-Kutta method are used as the time step method. The NURBS based BEM method is used to calculate the velocity potential at each time step. An artificial damping zone is adopted as the far field radiation condition on the free surface to avoid the wave reflection from the outer boundary.

Mathematical Models. A Cartesian coordinate system is used in this procedure. On the assumption that the fluid is inviscid and the flow is irrotational, the flow field can be described by a velocity potential function ϕ satisfying the Laplace equation:

$$\nabla^2\phi = 0 \tag{1.1}$$

The boundary conditions on the free-surface are given by:

$$\frac{\partial\eta}{\partial t} = \frac{\partial\phi}{\partial z} - \frac{\partial\phi}{\partial x}\frac{\partial\eta}{\partial x} - \frac{\partial\phi}{\partial y}\frac{\partial\eta}{\partial y} \tag{1.2}$$

$$\frac{\partial\phi}{\partial t} = -g\eta - \frac{1}{2}(\nabla\phi)^2 \tag{1.3}$$

Where Eq. 1.2 is the nonlinear kinetic free-surface condition and Eq. 1.3 is the dynamic free-surface condition. The boundary conditions applied on the body surface and seabed are given by:

$$\frac{\partial\phi}{\partial n} = U_n \qquad \text{on the body surface} \tag{1.4}$$

$$\frac{\partial\phi}{\partial n} = 0 \qquad \text{on the seabed} \tag{1.5}$$

in which U_n is the speed of body surface. And at far field, the velocity potential must satisfied appropriate radiation condition. A boundary integral equation based on the distribution of Rankine sources is used to solve Eq. 1.6.

$$C(p)\phi(p) + \iint_s \frac{\partial G(p,q)}{\partial n(q)}\phi(q)dS = \iint_s G(p,q)\frac{\partial\phi(q)}{\partial n(q)} \tag{1.6}$$

where,
$C(p)$ is the solid angle, $G(p,q)$ is the Rankine Green function, $p(x,y,z)$ is the field point and $q(x',y',z')$ is the source point. In every time step, the velocity potential ϕ on the free surface and the $\partial\phi/\partial n$ on the body surface are known. Then Eq. 1.6 can be solved and the velocity potential in the total fluid domain can be obtained.

The time derivative of velocity potential $\partial\phi/\partial t$ in above equation is obtained by solving a boundary integral equation. The value of $\partial\phi/\partial t$ should satisfy the Laplace equation in the fluid domain and the value of $\partial\phi/\partial t$ on the free surface is given in Eq. 1.3. The normal derivative of $\partial\phi/\partial n$ on the body surface can be obtained using the method given by Tanizawa (1995 and 2000) and by Cao et al. (1994).

Numerical Approach. A NURBS (*Non-Uniform Rational B-Spline*) based boundary element method is used to solve Eq. 1.6 and the NURBS surface is given by:

$$\vec{p}(u,v)=\frac{\vec{X}}{W}=\frac{\sum_{i=0}^{m}\sum_{j=0}^{n}w_{i,j}\vec{B}_{i,j}N_{i,k}(u)N_{j,l}(v)}{\sum_{i=0}^{m}\sum_{j=0}^{n}w_{i,j}N_{i,k}(u)N_{j,l}(v)} \quad (1.7)$$

in which $\vec{X}$ is the position vector along the surface as a function of the parameters *u* and *v*, $N_{i,k}(u)$ and $N_{j,l}(v)$ are the normalized B-spline basis function of degree *k* and *l* in the *u* and *v* directions, respectively; $w_{i,j}$ are the weights; $\vec{B}_{i,j}$ are the control point net. The distribution of velocity potential ϕ on the boundary surface is represented by the B-spline surface given by:

$$\phi(u,v)=\sum_{i=0}^{m}\sum_{j=0}^{n}\phi_{i,j}N_{i,k}(u)N_{j,l}(v) \quad (1.8)$$

The boundary integral in Eq. 1.6 can then be rewritten as:

$$\begin{aligned}&C(p)\sum_{i=0}^{m}\sum_{j=0}^{n}\phi_{i,j}N_{i,k}(u_p)N_{j,l}(v_p)-\\&\iint_S\sum_{i=0}^{m}\sum_{j=0}^{n}\phi_{i,j}N_{i,k}(u_q)N_{j,l}(v_q)\frac{\partial G(p,q)}{\partial n}dS(q)\\&=-\iint_s G(p,q)\sum_{i=0}^{m}\sum_{j=0}^{n}\phi_{i,j}N_{i,k}(u_q)N_{j,l}(v_q)dS(q)\end{aligned} \quad (1.9)$$

where,
$\phi_{i,j}$ are the unknown values. Applying Gaussian quadrature to carry out the integrations and the Galerkin method to set up the linear system equations, the equation can be solved numerically. In the case of a flat bottom, image sources can be used to eliminate the integration over the bottom surface. The Green function is given by:

$$G(p,q)=\frac{1}{R_1}+\frac{1}{R_2}+\frac{1}{R_3}+\frac{1}{R_4} \quad (1.10)$$

in which *R* expresses the distance between source and field points corresponding their images respectively.

A time-step method is used to calculate the fluid field at next time step. The time derivative of position and potential of the free surface is:

$$\frac{D\phi}{Dt}=f(t)=-g\eta+\frac{1}{2}\nabla\phi\cdot\nabla\phi \quad (1.11)$$

$$\frac{DX}{Dt}=g(t)=\nabla\phi \quad (1.12)$$

The fourth order Runge-Kutta scheme is employed in the first four time-steps. Using a 4th order Adams-Bashforth-Moulton predictor-corrector method, the calculation is carried out to the next time step. After each time step, the intersection of free-surface and body surface will change, the new position of intersection can be achieved by tracing the motion of intersection on the body surface. The grid on the body surface is corrected after the position of intersection has been achieved.

To ensure the stability of the calculation, the grid on free-surface is reformed after a number of time steps and a filter procedure is used to the point on the free-surface to avoid the saw-tooth phenomenon. A seven point filter method given by Huang (1997) is used to this point on the free-surface.

$$\bar{f}_i=\sum_{j=-3}^{3}\omega_i f_{i-j} \quad (1.13)$$

where,
$\bar{f}_i$ is the result of the filter procedure,
ω_i is the coefficient given, being 0.701207, 0.230696, -0.100604, and 0.019361 respectively.

An artificial damping zone is used for open boundary conditions. The form of the artificial damping term in the dynamic and kinematic free surface boundary condition is:

$$\frac{\partial \eta}{\partial t} = \frac{\partial \phi}{\partial z} - \frac{\partial \phi}{\partial x}\frac{\partial \eta}{\partial x} - \frac{\partial \phi}{\partial y}\frac{\partial \eta}{\partial y} - \nu(x)\eta \qquad (1.14)$$

$$\frac{\partial \phi}{\partial t} = -g\eta - \frac{1}{2}(\nabla\phi)^2 - \nu(x)\frac{\partial \phi}{\partial n} \qquad (1.15)$$

$$\nu(x) = \begin{cases} \alpha\left[1 - \cos\dfrac{\pi(x - x_0)}{(L - x_{0)}}\right] & x_0 \le x < L \\ 0 & x < x_0 \end{cases} \qquad (1.16)$$

where,
$\nu(x)$ is the damping term; L is the length of the tank and x_0 is the start point of damping zone; α is a coefficient to control the strength of the damping zone. The length of the damping zone is one and half wave length and the coefficient α is set to be 1.0.

Computational Result. The test is about the wave propagation in the wave tank. The dimension of tank is 5.0m water depth, 40m width and 100m length. On the left side of the tank is the piston style wave maker. The motion amplitude of the wave maker is 0.1m and the period is 3.0s. The damping zone is placed on the free surface near the right side of the tank with the length of 20m. Totally 4294 unknowns are used in the computation. The shape of free surface at different time are shown in Figs. 1.1 and 1.2. The wave elevations at a given point with different time step sizes are recorded in Fig. 1.3. The effect of damping zone is test by comparing the time history for surface elevation at a point on the central line of the tank with X=80m with or without a damping zone. The result is shown in Fig. 1.4 and the effect of damping zone is shown to be good.

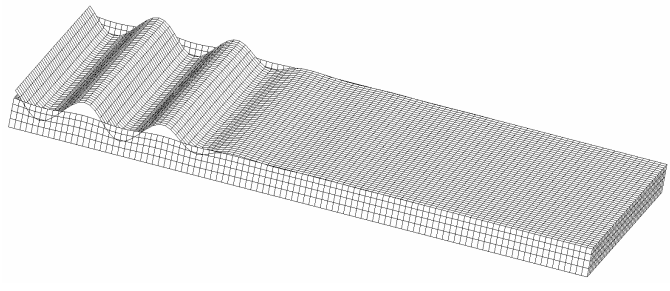

Figure 1.1- Free surface in the numerical wave tank at t=5.0T.

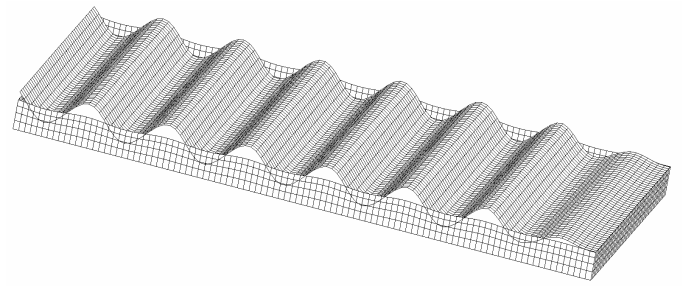

Figure 1.2- Free surface in the numerical wave tank at t=15.0T.

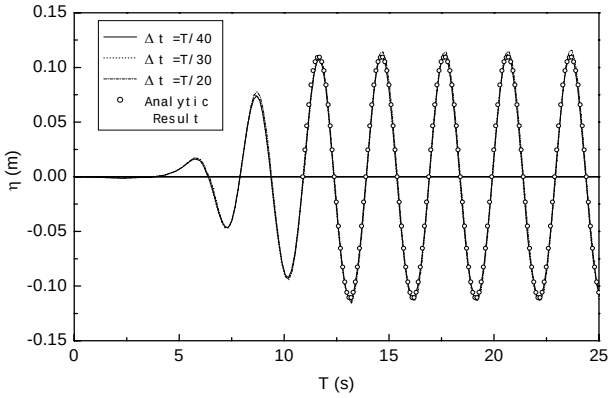

Figure 1.3- Time history of surface elevation at point X=20m.

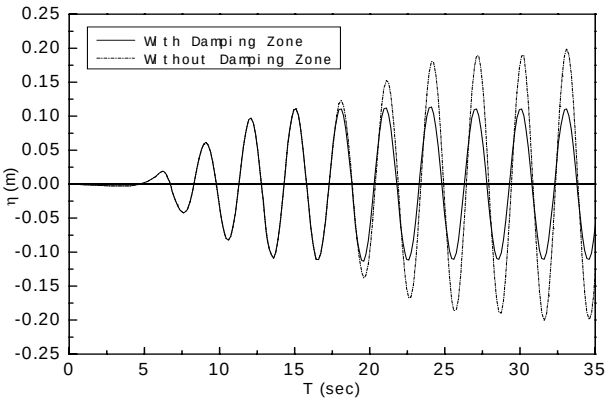

Figure 1.4- Comparison of time history for surface elevation at point X=80m with or without damping zone.

A bottom-mounted vertical circular cylinder is placed in the wave tank. The radius *a* of the cylinder is 1.0m. The depth *d* of the water is equal to *a*. The wave height $H = 0.06\lambda$, where λ is the wavelength. The time history of the horizontal wave force on the cylinder for $ka = 1.0$ is shown in Fig. 1.5. The wave field

around the cylinder is shown in Fig. 1.6. The maximum horizontal wave forces on the cylinder in waves with different wavelengths are shown in Fig. 1.7. The results are compared with the linear analytic result given in MacCamy and Fuchs (1954) and the nonlinear effect is shown to be significant.

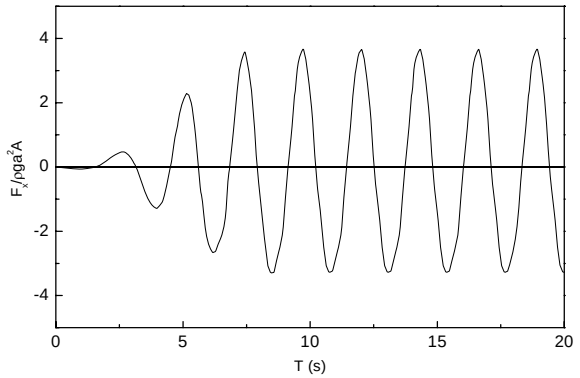

Figure 1.5- Time history of horizontal wave force on a bottom-mounted vertical cylinder, $ka = 1.0$.

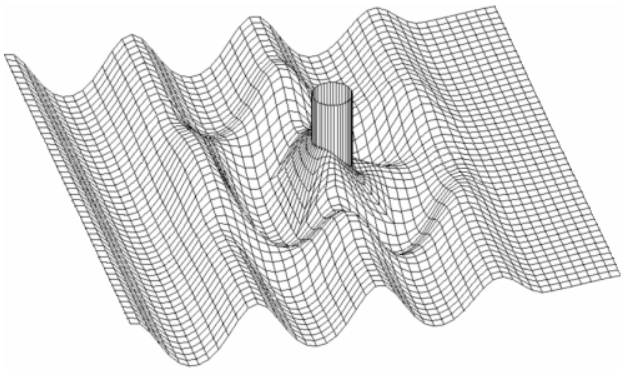

Figure 1.6- Oblique views of free surface profile around a circle cylinder, $ka = 1.0$.

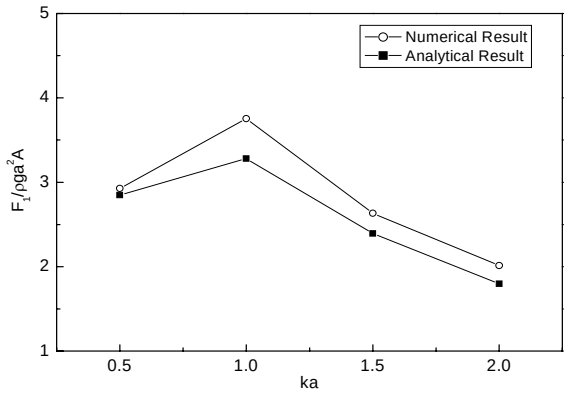

Figure 1.7- Maximum horizontal wave force on a bottom-mounted vertical cylinder.

Concluding Remarks. A fully non-linear method is developed for studying the interaction between 3-D body and waves. The boundary integral equation is solved using the numerical models of high-order NURBS based boundary element method and a mixed Eulerian-Lagrange scheme for the free-surface condition is employed. The wave propagation in a numerical wave tank is calculated as a test. The computational result of the wave elevation and hydrodynamic force on a vertical cylinder agree well with the analytic result. An iterative method is used in the calculation of the pressure on the surface of floating body in water and the results of forces and motions are shown to be accurate.

References.

Cao, Y., Beck, R. and Schultz, W.W., 1994, "Nonlinear Computation of Wave Loads and Motions of Floating Bodies in Incident Waves", Proc. of 9th International Workshop on Water Waves and Floating Bodies, pp 33-37.

Huang, Y.F., 1997, "Nonlinear ship motions by a Rankine panel method", PhD thesis, MIT, pp 60-63.

MacCamy, R.C. and Fuchs, R.A., 1954, "Wave force on piles: A diffraction theory", Technology Memo No. 69, US Army Corps of Engineers, Beach Erosion Board.

Tanizawa, K., 1995, "A nonlinear simulation method of 3D body motions in waves", Journal of Society of Naval Architecture Japan, Vol 178, pp 179-191.

Tanizawa, K., 2000, "The State of the Art on Numerical Wave Tank", Proc. 4th Osaka Colloquium on Seakeeping Performance of Ships, pp 95-114.

1.5 Discussion to the 24th ITTC Ocean Engineering Committee by Yanying Wang and Jiwen Xu, Dalian University of Technology, China, on Application of Wavelet Approach to Wave Spectral Analysis

Wavelet analysis is a relatively new technique. It has been implemented in many fields such as image processing, numerical analysis and communication theory. But its application to ocean engineering and oceanography is rare. Here, a wavelet transform is used to analyze the spectrum of a series of data and the results are compared with that of FFT methods.

The data is from North Alwyn platform in the northern North Sea and was recorded during a long storm in November 1997. The data comprise surface elevation measurements in the storm from one altimeter. Each sample contains 20 minutes (6000 data points) of the time series and the data contains 409 samples.

Wavelet Analysis. Wavelet transforms can be considered a broadened extension of the commonly used Fourier transform. Rather than sine, cosine, the basis functions of wavelet transform are called mother wavelets. The mother wavelets must satisfy several properties, such as:

- The amplitudes must decay rapidly to zero,
- The wavelets must have zero mean.

The wavelet transform (WT) of the signal, x(t), is defined as followed:

$$WT(\tau,b)=\int_{-\infty}^{\infty}x(t)g_{\tau b}^{*}(t;\tau,b)dt \qquad (1.17)$$

$g_{\tau b}$ is called translated and dilated wavelets, which is generated from mother wavelet g(t):

$$g_{\tau b}(t;\tau,b)=\frac{1}{\sqrt{b}}g(\frac{t-\tau}{b}) \qquad (1.18)$$

where,
τ is the transform parameter,
b is the scale dilation parameter.

Considering the properties of ocean waves, Morlet's wavelet can be used to analyze oceanic signals (Goupillaud et al., 1984):

$$g(t)=\exp(-\frac{1}{2}t^{2})\exp(ict) \qquad (1.19)$$

The wavelet transform conserves the total energy, which is:

$$\int_{-\infty}^{\infty}|x(t)|^{2}\,dt=C^{-1}\int_{0}^{\infty}\int_{0}^{\infty}|WT(\tau,b)|^{2}\,b^{-2}d\tau db \qquad (1.20)$$

in which the coefficient C is given by Eq. 1.17.

Based on Eq. 1.20, we can deduce the time-spectrum frequency spectrum, time spectrum, and frequency spectrum. Here we just compute the frequency spectrum to make a comparison with that of the FFT method.

FFT Analysis. The FFT algorithm is a conventional method to analyze energy spectrum in ocean engineering. Its properties of fast computing speed and precise spectrum amplitude results make it commonly used. But sufficiently long time series are necessary when using the FFT method.

Comparison. For comparison, 2 samples with different sample lengths from the medium period of the storm are analyzed by both methods. The results are shown in Figs.1.8 to 1.13.

It can be found that with decreasing sample length the FFT spectrum becomes malformed. The amplitudes and spectrum peak frequencies differ a lot. Otherwise, the change of sample length does not influence the wavelet spectrum greatly.

According to the spectra, statistics of the ocean waves can be conveniently found, which are listed in Tables 1.1 and 1.2.

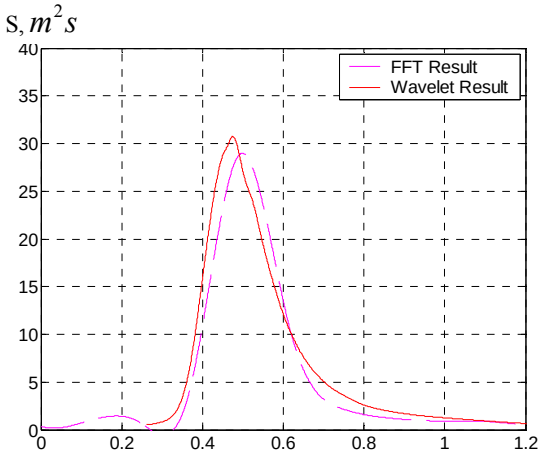

Figure 1.8- The energy spectral density functions for 200th sample with 6000 data points.

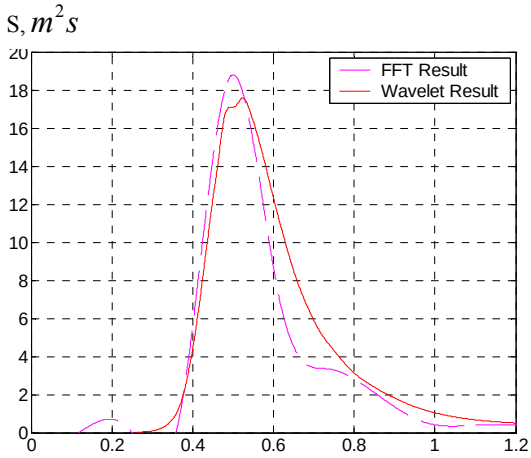

Figure 1.11- The energy spectral density functions for 250th sample with 6000 data points.

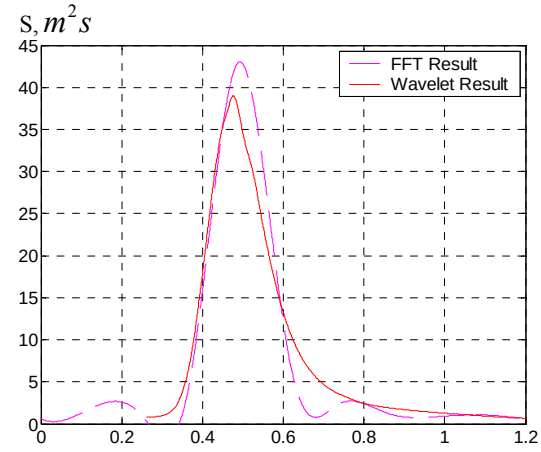

Figure 1.9- The energy spectral density functions for 200th sample with 3000 data points.

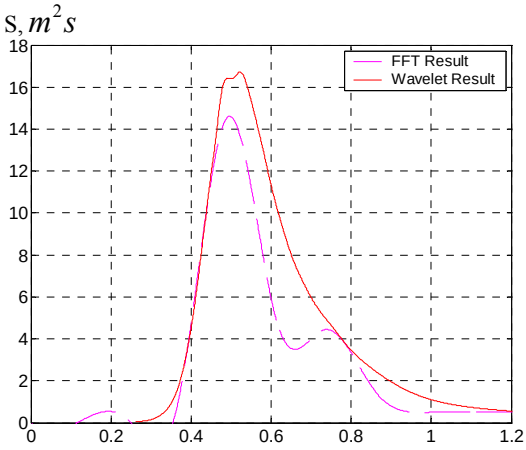

Figure 1.12- The energy spectral density functions for 250th sample with 3000 data points.

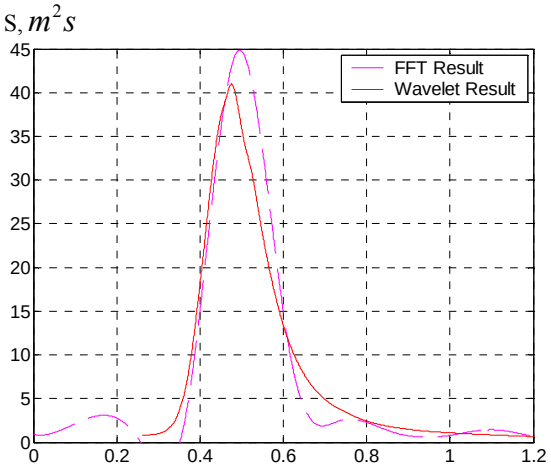

Figure 1.10- The energy spectral density functions for 200th sample with 2000 data points.

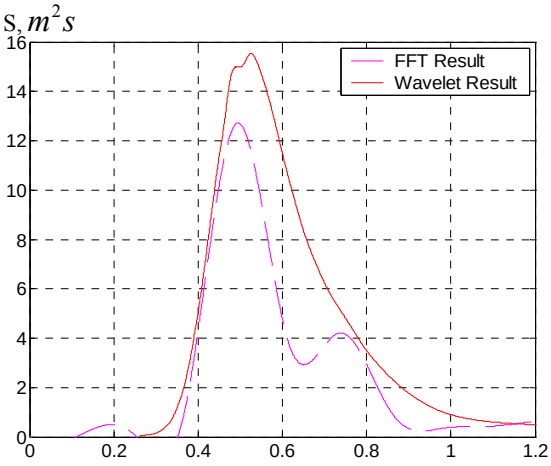

Figure 1.13- The energy spectral density functions for 250th sample with 2000 data points.

Table 1.1- Comparison of Statistics of 200th Sample.

Sample length	Method	Hs (m)	Tz (s)	t1 (s)	Tp (s)
6000	FFT	10.17	10.00	11.08	12.59
	Wavelet	10.65	8.42	10.52	13.22
3000	FFT	11.42	10.43	11.60	12.76
	Wavelet	11.42	8.70	10.77	13.20
2000	FFT	11.76	10.48	11.59	12.69
	Wavelet	11.53	8.86	10.88	13.20

Table 1.2- Comparison of Statistics of 250th Sample.

Sample length	Method	Hs (m)	Tz (s)	t1 (s)	Tp (s)
6000	FFT	8.19	9.35	10.19	12.56
	Wavelet	8.89	7.52	9.53	12.00
3000	FFT	7.53	9.08	9.89	12.66
	Wavelet	8.82	8.01	9.56	12.02
2000	FFT	7.05	8.96	9.84	12.69
	Wavelet	8.71	8.02	9.60	11.95

Suggestion. Because of the wavelet's property of tight frame, the wavelet method is more suitable for a small sample spectrum computation than the FFT method. Moreover, wavelet approach has a good capability to analyze signals in the time-frequency domain. Therefore, the application of the wavelet in the time-frequency domain should be explored. The following are some of the probabilities of wavelet application:

1. Forecast wave properties according to small wave data,
2. Compute ocean wave's time-frequency spectrum,
3. Find the tendency of frequency changing with time.

References.

Daubechies, I., 1992, "Ten Lectures on Wavelets", Society for Industrial and Applied Mathematics.

Goupillaud, P., Grossmann, A. and Morlet, J., 1984, "Cycle-octave and related transforms in seismic signal analysis", Geoexploration, 23, 85-102.

Liu, P.C., 2000, "Is the wind wave frequency spectrum outdated", Ocean Engineering, 27, 577-588.

Wang, Y., Xu, J. and Liang, H.E., 2002, "A Discussion on Application of JONSWAP Spectral Function to Wave Data Analysis for Storm 149 from North Alwyn", 23rd ITTC, Venice, Italy.

Wolfram, J., 2001, "Storm Wave Data from North Alwyn", Academic exchange letter from the SCW, 23rd ITTC, November.

2. COMMITTEE REPLIES

2.1 Reply of the 24th ITTC Ocean Engineering Committee to Neil Bose

We would like to thank Prof. Bose for his questions. With respect to the wind farm issue, we have been informed by the authors of the original paper (Inoue et al., 2005) that wind drag acting on the farm should be balanced in order to avoid drifting of the farm. Lift force on the sails thrusts the farm and lift force on the keels of the farm balances the wind drag. It means that the farm mainly sails in a beam condition. Their simulations also confirmed that the wind farm can operate mostly in a good breeze and safely escape from a typhoon.

With respect to laboratory wind modelling, we first refer to Section 3.4 in our Report, where concluding remarks from our Committee work on this issue are given. When it comes to particular improvements that should be made, as requested by Prof. Bose, we want to point out the need for more standard procedures, or more commonly accepted references. We also believe that in general, the use of arrays of external fans is the preferred generation procedure, although there may be some cases where alternative methods will be preferred.

Furthermore, basic experimental studies to validate the use of Froude scaling, and documentation of deviations, are needed for various types of vessels and superstructures, and for various headings. Shielding and damping effects should also be investigated in more detail. The interaction from waves on the wind near the surface is another issue to look into. Finally, we want to emphasize that wind modelling in a wave basin is not, and cannot be, as accurate as in a wind tunnel, and this must be kept in mind.

The need for further work, as reflected in the above comments, is being brought forward as one of the tasks for the 25th ITTC Ocean Engineering Committee.

References.

Inoue, K., Tanaka, S., Kinoshita, T., Takagi, K., Terao, Y., Okamura, H., Takahashi, M., Esaki, H. and Uehiro, T., 2005, "Development of a Floating Wind Farm with Mooringless System", Proc. 18th Ocean Engineering Symposium, CD-ROM.

2.2 Reply from the 24th ITTC Ocean Engineering Committee to Bruce Johnson

We appreciate Dr. Johnson's comments where he points out the recent strong development within the methods and data on field wave observations, in particular radar measurements. Together with theoretical models, field data are essential in establishing a basis for physical and numerical modelling. The referred EU MaxWave project represents a noticeable step forward in this field, in particular within space-borne and ship-borne radar measurements providing space-time information rather than only single point measurements.

The project is already mentioned briefly in our Report, Section 2.2, by a reference to Nieto Borge et al. (2003), while we agree that the more detailed comments given by Dr. Johnson are also relevant for the Report. An overall project summary is given by Rosenthal (2005). We find that in particular, the observation of wave group propagation and possible non-linear behaviour that could in some cases lead to extreme events, is interesting, as it describes phenomena that may be relevant for numerical and physical modelling. The same problem has also been studied through laboratory measurements, see Stansberg (2000, 2003), and comparisons to field data will be of great value.

In addition to the wave group studies, one problem that was particularly studied in the MaxWave project was the possible accurate observation of extreme individual wave and crest heights from spatial or ship-borne radar observations, see Lehner (2005). As we have interpreted the findings, one has significantly improved the methodology in use of such data for this purpose, and there is a great potential for the future in this. At present, however, the accuracy needs still to be documented through extensive calibrations before practical use, which is a challenging task as discussed in Muller et al. (2005). Also, one should recall the challenge in that a large amount of good quality data is required to establish reliable statistics for extremes from field data, due to the considerable sampling variability. Finally, we also mention that the MaxWave work has initiated new efforts in the investigation of the statistics in a spatial domain, see Krogstad et al. (2004).

A lot more could be said about the MaxWave data as such and the related technology development. We feel, however, that an even broader and more detailed description of these matters may be more relevant for ISSC (International Ship and Offshore Structures Congress) than for ITTC where we primarily focus on the modelling issues. But one might perhaps address whether or not the actual technology could be transformed to small-scale measurements in a laboratory?

References.

Krogstad, H., Socquet-Juglard, H., Dysthe, K.B. and Trulsen, K., 2004, "Spatial Extreme Value Analysis of Nonlinear Simulations of Random Surface Waves", Proc. 23rd OMAE, Vancouver, Paper No. 515336.

Lehner, S., 2005, "Extreme Wave Statistics from Radar Data Sets", in Rogue Waves, Proc. of the 14th 'Aha Huliko'a Hawaiian Winter Workshop, 2005, pp. 9-14.

Muller, P., Osborne, A.R. and Garrett, C., 2005, "Rogue Waves", in Rogue Waves, Proc. of the 14th 'Aha Huliko'a Hawaiian Winter Workshop, 2005, pp. 185-193.

Nieto Borge, J.C., Niedermeier, A., Lehner, S. and Rosenthal, W., 2003, "Determination of Wave Field Properties in the Spatial Domain from Space Borne SAR Images", Proc. 21st OMAE, Cancun. Paper No. 37403.

Rosenthal, W., 2005, "Results of the MaxWave Project", in Rogue Waves, Proc. of the 14th 'Aha Huliko'a Hawaiian Winter Workshop, 2005, pp. 1-7.

Stansberg, C.T., 2000, "Nonlinear Extreme Wave Evolution in Random Wave Groups", Proc. 10th ISOPE Conf., Seattle, USA.

Stansberg, C.T., 2003, "Second- and Higher Order Effects in Steep Random Waves", Proc.12th ISOPE, Honolulu, Hawaii, USA.

2.3 Reply from the 24th ITTC Ocean Engineering Committee to Martin Renilson

The Committee wishes to thank Dr. Renilson for his interest in this topic which we think needs increased attention from those involved in large testing tanks and basins. Our main message in this context is that narrow-band uni-directional wave spectra show a non-homogenous behaviour with a frequency downshift during propagation over a long range corresponding to approximately 20 to 40 wave-lengths, and that this has been documented experimentally as well as theoretically (Stansberg, 1995 and Dysthe et al., 2003). Thus, it is not a laboratory determined effect, but rather an effect due to higher-order wave-wave interactions, which in the latter reference are modelled by a Modified Nonlinear Schrödinger (MNLS) equation. Also, the referred theoretical work documents a prediction of the f^{-4} trend in the spectrum tail. The topic was also addressed previously in the 22nd and 23rd ITTC Reports (the Environmental Modelling and Waves Committees, respectively), but the new results show the effects clearer than before.

Among the results shown in our presentation at the 24th ITTC were also some recent, yet unpublished, experimental data from MARINTEK's 270m long towing tank, as well as new numerical results in Socquet-Juglard et al. (2005). These are shown in Figs. 2.1 and 2.2 below, respectively. In the experiment, measurements were made at 10m, 80m, 120m and 160m distances from the wavemaker. The spectra in Fig. 2.1 are quite similar to those in Stansberg (1995), which were run at a smaller scale and in a wide basin instead of a long tank. This supports the statement that it is not a laboratory determined effect. Notice that the sea state of the actual experiment in Fig. 2.1 was quite steep, with some dissipation occurring in addition to the wave-wave interaction.

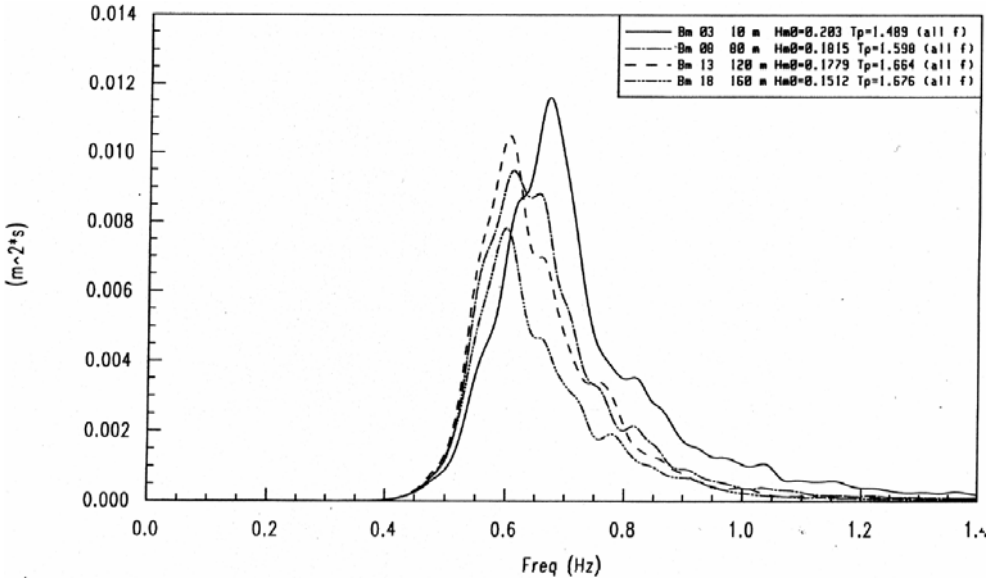

Figure 2.1- Example from spectra measured at four different locations in a 270m long tank. The initial wave frequency was 0.67Hz.

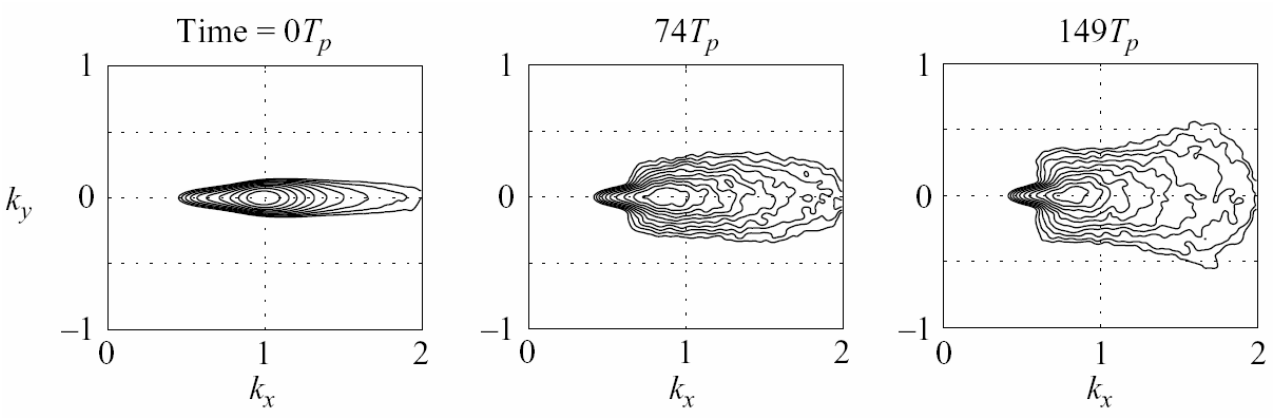

Figure 2.2- Contour plots showing wave number spectra at different evolution stages, for an almost unidirectional, narrow-band sea state (numerical simulations). $k_X = 1$ indicates the initial peak wave number. (From Socquet-Juglard et al., 2005, reproduced by permission from Cambridge University Press).

The new results in Fig. 2.2 are based upon the same model as in the earlier work, Dysthe at al. (2003). The results are shown as functions of the wave number rather than frequency, at different stages of the evolution. We have not made any detailed and quantitative comparison to the experimental results, but one can clearly see that the frequency downshift trends are qualitatively similar. Further work is recommended on this topic.

One should also note that the higher-order spectral evolution is connected with non-linear group formations that can lead to abnormal extreme wave events, as discussed by Onorato et al. (2004) as well as in Socquet-Juglard et al. (2005) and also addressed in Section 2.2 in our Report.

References.

Dysthe, K.B., Trulsen, K., Krogstad, H.E. and Socquet-Juglard, H., 2003, "Evolution of a

Narrow Band Spectrum of Random Surface Gravity Waves", Journal of Fluid Mechanics, Vol. 478, 1-10.

Onorato, M., Osborne, A.R., Serio, M., Cavaleri, L., Brandini, C. and Stansberg, C.T., 2004, "Observation of Strongly Non-Gaussian Statistics for Random Sea Surface Gravity Waves in Wave Flume Experiment", Physical Review E, Vol. 70, 067302:1-4.

Socquet-Juglard, H., Dysthe, K., Trulsen, K., Krogstad, H.E. and Liu, J., 2005, "Probability Distributions of Surface Gravity Waves During Spectral Changes", Journal of Fluid Mechanics, Vol. 542, pp.195-216.

Stansberg, C.T., 1995, "Effects from Directionality and Spectral Bandwidth on Nonlinear Spatial Modulations of Deep-Water Surface Gravity Wave Trains", Proc. 24th ASCE International Conference on Coastal Engineering, Vol. 2, Kobe.

2.4 Reply from the 24th ITTC Ocean Engineering Committee to Yanying Wang and Kun Qian

The Committee would like to thank both authors for their interesting contribution. The proposed method belongs to the family of mixed Eulerian-Lagrangian methods (MEL) for the time domain solution of potential flows with non-linear free-surface conditions. Besides the recent development of methods such as VOF, Level Set, CIP, or particle approaches such as MPS or SPH , which have the capacity to simulate complex free surface flows including wave breaking and interface reconnection, there is room for reliable non-linear free-surface potential flow codes. Such tools may give results of high interest for example in terms of higher order diffraction forces on offshore structures, with possibly less computational power requirements than the above-mentioned CFD approaches.

Consequently, the Committee would like to encourage the authors of this discussion to publish their work in refereed scientific journals, including validation of their results versus established numerical or experimental benchmark data for non-linear effects. Another important aspect is also robustness which is a strong point of VOF-type or SPH methods, and may sometime be problematic with 3D MEL methods. This robustness is to be documented for example by simulating highly non linear (but non-breaking) diffraction flows.

2.5 Reply from the 24th ITTC Ocean Engineering Committee to Yanying Wang and Jiwen Xu

The Ocean Engineering Committee wishes to thank Profs. Wang and Xu for their contribution on applying Wavelet transformation in the analysis of field wave data. We agree that this new technique can be helpful in the analysis of various types of data including wave measurements, from the ocean as well as in the laboratory. In particular, we understand that it is a convenient tool in the interpretation of extreme events or non-stationary and transient phenomena, such as described in Lin and Liu (2004).

In the above discussion by Wang and Xu, the method is applied to estimate the spectral shape from short time series samples. Their estimates appear to be smoother than corresponding estimates from conventional Fourier analysis, which show a fluctuating behaviour due to the short records. We believe that the actual problem does not necessarily have any unique solution, due to natural sampling variability, leading to an inherent uncertainty connected with the spectrum estimation. Therefore, it is difficult to conclude whether the Wavelet method, as such, is superior to the Fourier method or not in this specific application.

The fact that the Wavelet method gives smoother results seems to be a result of a larger

degree of frequency smoothing, due to the time-domain Morlet window modulation. Thus it acts like a filter on the spectrum variation vs. frequency. If this is the case, the issue is perhaps rather a higher (and possibly preferable) degree of smoothing, than the Wavelet methodology in itself.

In any case, we agree that the method can be a good alternative to the conventional procedures for short records. We recommend that calibrations on numerical synthetic records should be done to clarify possible artificial effects ("fingerprints") from the Wavelet filtering procedure.

References.

Lin, A.B. and Liu, P.C., 2004, "A discrete wavelet analysis of freak waves in the ocean", Journal of Applied Mathematics, 2004:5,379-394), (http://www.glerl.noaa.gov/pubs/fulltext/2004/20040032.pdf)